Analysis of effects of the state of charge on the formation and growth of the deposit layer on graphite electrode of pouch type lithium ion polymer batteries

CrossMark

Victor A. Agubra [a,*], Jeffrey W. Fergus [a], Rujian Fu [b], Song-Yul Choe [b]

[a] Materials Research and Education Center, Auburn University, 275 Wilmore Laboratories, Auburn, AL 36849, USA
[b] Department of Mechanical Engineering, Auburn University, 1418 Wiggins Hall, Auburn, AL 36849, USA

HIGHLIGHTS

- Raising the battery state of charge increased the rate of side reaction.
- A significant amount of lithium was consumed in forming the deposit layer.
- Loss of carbon particles adhesion led to particles isolation in the electrochemical process.

ARTICLE INFO

ABSTRACT

The breakdown of the protective solid electrolyte interface (SEI) layer formed on lithium ion battery anodes can initiate further electrolyte decomposition and the formation of non-uniform and electronically insulating reaction products on the surface of the graphite particles. The results from this study indicate that raising both the lower and upper ends of the state of charge (SOC) increased the rate of the electrolyte decomposition side reaction to form a thick deposit surface film. This deposit layer contained lithium that can no longer participate in the reversible electrochemical reaction. In addition, the high cycling potential coupled with high charge rate created a large lithium concentration gradient that led to some particles detachment from the current collector and isolation in the electrochemical process.

1. Introduction

Cost effective implementation of lithium ion batteries requires long operational lifetimes, so various research groups have been exploring mechanisms that cause the lithium ion battery to lose its capacity [1–8]. Mechanisms such as loss of accessible lithium ions, degradation of electrodes, binder, corrosion of current collectors, and electrolyte decomposition to form an insoluble film between electrode and electrolyte interface have been reported as some of the main contributing factors to capacity fade [9–11].

A robust SEI layer prevents the occurrence of further electrolyte reduction on the carbon electrode, which is formed from the reduction of the electrolyte salt $LiPF_6$ to produce a strong Lewis acid PF_5 [12] that undergoes a ring-opening reaction with the solvent molecules in the presence of the Li^+ to initiate its formation. This SEI layer is a Li^+ conductor but an insulator to electron flow. However, at elevated temperature the metastable species $ROCO_2Li$ within the SEI layer decomposes into more stable compounds $-Li_2CO_3$ and LiF, which distort the SEI layer [13] and create a porous SEI structure that exposes the graphite surface to more electrolyte decomposition reaction [14]. The deposited layers lead to the loss/consumption of recyclable lithium ions at electrode/electrolyte interface and are one of the major causes of reversible capacity loss in the lithium ion battery.

In this article, a quantitative analysis of the effect of the state of charge (SOC) on the growth of the deposit layer on the anode electrode/electrolyte interface and a direct measurement of the loss of carbon particles resulting from diffusion induced stress during the intercalation/de-intercalation of lithium ion into the graphite structure are presented. The deposition due to solvent reduction

was observed only at the graphite electrode that on the cathode was considered negligible. Understanding the effects of the deposit layer on the lithium kinetics at the electrode/electrode interface and performance degradation is important.

2. Experimental

2.1. Battery chemistry

The batteries used in this study were the large format pouch type-lithium ion polymer batteries from battery manufacturer LGChem with a Li(Mn,Ni,Co)O_2 cathode and the anode material made of carbon with polyvinylidene fluoride (PVDF) as the binding material, with a composition of less than 3 wt% of the active material. The current collectors for anode and cathode electrode were copper and aluminum metals respectively. The batteries had a polymer electrolyte that consist of polyethylene oxide with lithium salt, $LiPF_6$, with co-solvents of ethylene carbonate (EC), and dimethyl carbonate (DMC). The nominal capacity of each battery is 15.7 Ah with an operating voltage level of 2.5–4.15 V. The complete battery were provided by the General Motors Company Ltd.

2.2. Cycling test

The charge/discharge cycles were performed using a in-house designed test station that comprised of a programmable charging system, a programmable electronic load system, a data acquisition system that are controlled by LabVIEW™ residing in a PC. The testing system allowed for the input of various charging conditions, such as C-rate, state of charge (SOC), and was located in an environmental chamber to allow for control of the external temperature. The batteries were charged by a constant current-constant voltage (CC–CV) charging protocol at room temperature. In each cycle, the cell was discharged with a constant current until the terminal voltage decreased to the voltage corresponding to the desired lower SOC and then charged with a constant current up to the voltage corresponding to the upper SOC followed by a constant voltage (CV) charge. A 4C charge and discharge current were used to accelerate the aging process. After every 20 cycles, a 1C discharge–resting–charge profile was applied to the cell to measure its capacity. The capacity (Q_{max}) was calculated by integrating the current when the cell was being discharged from 100% to 0% SOC using 1C current (15.7A) at room temperature. The Q_{max} data for each battery were recorded every 20 cycles. The battery was rested for 10 min before and after the Q_{max} measurement. The SOC levels; 5–70%, 15–80% and 25–90% were chosen to maintain a constant capacity of 65%. The pre-test terminal voltage for the desired SOC was determined by coulomb counting.

2.3. Electrochemical impedance spectroscopy (EIS)

A Gamry electrochemical impedance spectroscopy (EIS) framework in galvanostatic mode was used to apply different frequencies (1 mHz–1 kHz) of small AC excitation current (1 A) to battery and voltage responses were collected at 25 °C. The battery state of charge was maintained at 50% during the EIS test. A bipolar power supply was used to amplify the signal from EIS signal board. The measured impedances of the batteries were fit using the equivalent circuit model shown in Fig. 1 to find parameters such as the SEI film resistance, the Ohmic resistance, the charge transfer resistance, the double layer capacitance and Warburg impedance of the battery. In the model, R_0 presents the Ohmic resistance caused by electrolyte, deposit layer, separator, current collector and electrode, which equals to the left intercept between impedance spectrum and the x-
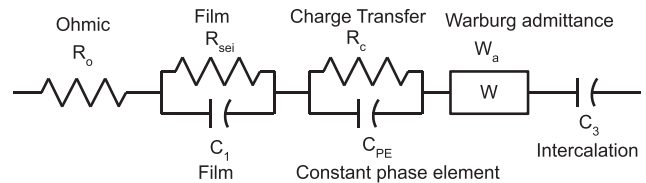

Fig. 1. Equivalent circuit model.

axis at high frequency ($\approx$ 1 kHz) [2]. R_{sei} and C_1 indicate SEI resistance and constant phase element (CPE) at anode [3], which dominate the shape of the first semi-circle in high frequency domain from 1 kHz to several Hz [4]. While R_c and C_2 indicate charge transfer resistance and double layer capacitance, respectively. They affect the shape of the second semi-circle, which is less obvious in the lower frequency range (several Hz to several mHz) [3]. On the other hand, W_a is the Warburg admittance represents ion diffusion in the solid electrode and C_3 is the intercalation capacitance that indicates the process of ion intercalation [3]. Both W_a and C_3 dominate the impedance spectrum in the low frequency region (<several mHz). To extract these parameters, the EIS-ECM was fitted to the impedance spectrum measured by EIS using simplex algorithm.

2.4. Materials postmortem analysis

After cycling the batteries for 600 cycles and measurement of capacity and impedance, the battery was discharged to 0% SOC and dismantled in an argon atmosphere in glove box. The anode electrodes were harvested, cleaned in DMC and dried. A quantitative analysis of the thickness of the formed deposit layer was carried out by taking a cross sectional view (the samples were mounted on an epoxy and the edges polished) of the deposited surface layer and measuring its thickness using a scanning electron microscope (SEM) (Fig. 2). Four anode electrodes (out of a total 13 electrodes) from each condition were selected by visual examination to represent the range of the amount of deposit and area of carbon particles loss. Specifically, one electrode (out of 4) with heavy amounts of deposit/large area of carbon loss, one electrode (out of 3) with light amounts of deposit/small area carbon loss and two electrodes (out of 6) in-between these two extremes. Four samples were taken from each of the four selected electrodes, and for each sample, six different thicknesses of the deposited layer for each sample were measured. Therefore for each electrode, the thickness of the deposited layer was calculated by taken the mean value of the 24 measured thicknesses. Similarly, for the carbon particles loss area, the same numbers of electrodes and samples were used. The areas were measured by fitting the loss area with discrete circles or rectangles using annotate/measurement tool on the SEM. These areas were then calculated by averaging the areas of either the circles of the rectangles.

X-ray diffraction (XRD) spectra for the graphite anode electrode were obtained using a Bruker D8 to investigate the changes in the graphite crystal structure and the formation of any new phases. The composition of the deposit layer was also analyzed using Fourier transformed infra-red spectroscopy (FTIR) and X-ray photoelectron spectroscopy (XPS). For FTIR analysis, a Bruker optics equipped with single-reflection attenuated total reflection (ATR) accessory was used. The electrode samples were adjusted such that the beam was directly on the deposit layer area to ensure maximum absorbance. Each spectrum was recorded by accumulating 128 scans with a resolution of 4 cm. For XPS analysis, a VG ESCA scientific theta probe spectrometer was used.